

Determining the WIMP mass from a single direct detection experiment, a more detailed study

Anne M. Green[†]

[†] School of Physics and Astronomy, University of Nottingham, University Park, Nottingham, NG7 2RD, UK

E-mail: anne.green@nottingham.ac.uk

Abstract. The energy spectrum of nuclear recoils in Weakly Interacting Massive Particle (WIMP) direct detection experiments depends on the underlying WIMP mass. We study how the accuracy with which the WIMP mass could be determined by a single direct detection experiment depends on the detector configuration and the WIMP properties. We investigate the effects of varying the underlying WIMP mass and cross-section, the detector target nucleus, exposure, energy threshold and maximum energy, the local circular speed and the background event rate and spectrum. The number of events observed is directly proportional to both the exposure and the cross-section, therefore these quantities have the greatest bearing on the accuracy of the WIMP mass determination. The relative capabilities of different detectors to determine the WIMP mass depend not only on the WIMP and target masses, but also on their energy thresholds. The WIMP and target mass dependence of the characteristic energy scale of the recoil spectrum suggests that heavy targets will be able to measure the mass of a heavy WIMP more accurately. We find, however, that the rapid decrease of the nuclear form factor with increasing momentum transfer which occurs for heavy nuclei means that this is in fact not the case. Uncertainty in the local circular speed and non-negligible background would both lead to systematic errors in the WIMP mass determination. For deviations of $\pm 20 \text{ km s}^{-1}$ in the underlying value of the circular speed the systematic error is of order 10%, increasing with increasing WIMP mass. This error can be reduced by also fitting for the circular speed. With a single detector it will be difficult to disentangle a WIMP signal (and the WIMP mass) from background if the background spectrum has a similar shape to the WIMP spectrum (i.e. exponential background, or flat background and a heavy WIMP).

Keywords: dark matter, dark matter detectors

1. Introduction

Cosmological observations indicate that the majority of the matter in the Universe is dark and non-baryonic (e.g. Ref. [1]). Weakly Interacting Massive Particles (WIMPs) are one of the leading cold dark matter candidates, and supersymmetry provides a concrete, well-motivated WIMP candidate in the form of the lightest neutralino (e.g. Ref. [2, 3]). The direct detection of WIMPs in the lab [4] (see Ref. [5] for a review of current and future experiments) would not only directly confirm the existence of dark matter but would also allow us to probe the WIMP properties, as the shape of the differential event rate depends on the WIMP mass [6, 7, 8, 9, 10, 11]. Constraints on, or measurements of, the WIMP mass and elastic scattering cross-section will be complementary to the information derived from collider and indirect detection experiments [12].

In paper I [10], see also Refs. [9, 11], we examined the accuracy with which a future SuperCDMS [13] like direct detection experiment would be able to measure the WIMP mass, given a positive detection. In this paper we revisit that analysis, studying in more detail the dependence of WIMP mass limits on the detector capabilities (including threshold energy, exposure, maximum energy and target nucleus), the WIMP properties (mass and cross-section), the local circular speed and the effects of non-zero backgrounds. We outline the calculation of the differential event rate and the Monte Carlo simulations in Sec. 2 (see paper I [10] for further details), present the results in Sec. 3 and conclude with discussion in Sec. 4.

2. Method

2.1. Event rate calculation

The differential event rate, assuming spin-independent coupling, is given by (see e.g. [2, 6]):

$$\frac{dR}{dE}(E) = \frac{\sigma_p \rho_\chi}{2\mu_{p\chi}^2 m_\chi} A^2 F^2(E) \mathcal{F}(E), \quad (1)$$

where ρ_χ is the local WIMP density, σ_p the WIMP scattering cross section on the proton, $\mu_{p\chi} = (m_p m_\chi)/(m_p + m_\chi)$ the WIMP-proton reduced mass, A and $F(E)$ the mass number and form factor of the target nucleus respectively and E is the recoil energy of the detector nucleus. We use the Helm form factor [14]. The dependence on the WIMP velocity distribution is encoded in $\mathcal{F}(E)$, which is defined as

$$\mathcal{F}(E) = \left\langle \int_{v_{\min}}^{\infty} \frac{f^E(v, t)}{v} dv \right\rangle, \quad (2)$$

where $f^E(v, t)$ is the (time dependent) WIMP speed distribution in the rest frame of the detector, normalized to unity and $\langle \dots \rangle$ denotes time averaging. The WIMP speed distribution is calculated from the velocity distribution in the rest frame of the Galaxy, $f^G(\mathbf{v})$, via Galilean transformation: $\mathbf{v} \rightarrow \tilde{\mathbf{v}} = \mathbf{v} + \mathbf{v}^E(t)$ where $\mathbf{v}^E(t)$ is the Earth's

velocity with respect to the Galactic rest frame [6]. The lower limit of the integral, v_{\min} , is the minimum WIMP speed that can cause a recoil of energy E :

$$v_{\min} = \left(\frac{Em_A}{2\mu_{A\chi}^2} \right)^{1/2}, \quad (3)$$

where m_A is the atomic mass of the detector nuclei and $\mu_{A\chi}$ the WIMP-nucleon reduced mass. We use the ‘standard halo model’, an isotropic isothermal sphere, for which the local WIMP velocity distribution, in the Galactic rest frame, is Maxwellian

$$f^G(\mathbf{v}) = N [\exp(-|\mathbf{v}|^2/v_c^2) - \exp(-v_{\text{esc}}^2/v_c^2)] \quad |\mathbf{v}| < v_{\text{esc}}, \quad (4)$$

$$f^G(\mathbf{v}) = 0 \quad |\mathbf{v}| > v_{\text{esc}}, \quad (5)$$

where N is a normalization factor and $v_c = 220 \pm 20 \text{ km s}^{-1}$ [15] and $v_{\text{esc}} \approx 540 \text{ km s}^{-1}$ [16] are the local circular and escape speeds respectively. If the ultra-local WIMP distribution is smooth, then the uncertainties in the detailed shape of the local velocity distribution lead to relatively small changes in the shape of the differential event rate [17, 18]. Consequently there is a relatively small, [$\mathcal{O}(5\%)$], systematic uncertainty in the WIMP mass [10]. We caution that the assumption of a smooth ultra-local WIMP distribution may, however, not be valid on the sub milli-pc scales probed by direct detection experiments (e.g. Ref. [19] but see also Ref. [20] for arguments that the ultra-local WIMP distribution consists of a large number of streams, and is hence effectively smooth).

As shown by Lewin and Smith [6], see also Paper I [10], the differential event rate can, to a reasonable approximation, be written as

$$\frac{dR}{dE}(E) = \left(\frac{dR}{dE} \right)_0 \exp\left(-\frac{E}{E_R}\right) F^2(E). \quad (6)$$

The event rate in the $E \rightarrow 0 \text{ keV}$ limit, $(dR/dE)_0$, and E_R , the characteristic energy scale, are given by

$$\left(\frac{dR}{dE} \right)_0 = c_0 \frac{\sigma_D \rho_\chi}{\sqrt{\pi} \mu_{p\chi}^2 m_\chi v_c} A^2, \quad (7)$$

and

$$E_R = c_{E_R} \frac{2\mu_{A\chi}^2 v_c^2}{m_A}, \quad (8)$$

respectively, where c_0 and c_{E_R} are constants of order unity which are required when the Earth’s velocity and the Galactic escape speed are taken into account and are determined by fitting to the energy spectrum calculated using the full expression, eq. (1). The exact values of these constants depend on the target nucleus, the energy threshold and the Galactic escape speed. For a Ge detector with energy threshold $E_{\text{th}} = 0 \text{ keV}$, $c_0 \approx 0.78$ and $c_{E_R} \approx 1.72$, with a weak dependence on the WIMP mass [10]. For the majority of our calculations we will use the accurate expression, eq. (1), however in Sec. 3.3 where we consider varying v_c we will use the fitting function, eq. (6), as it is not computationally feasible to carry out the full calculation in the likelihood analysis in this case.

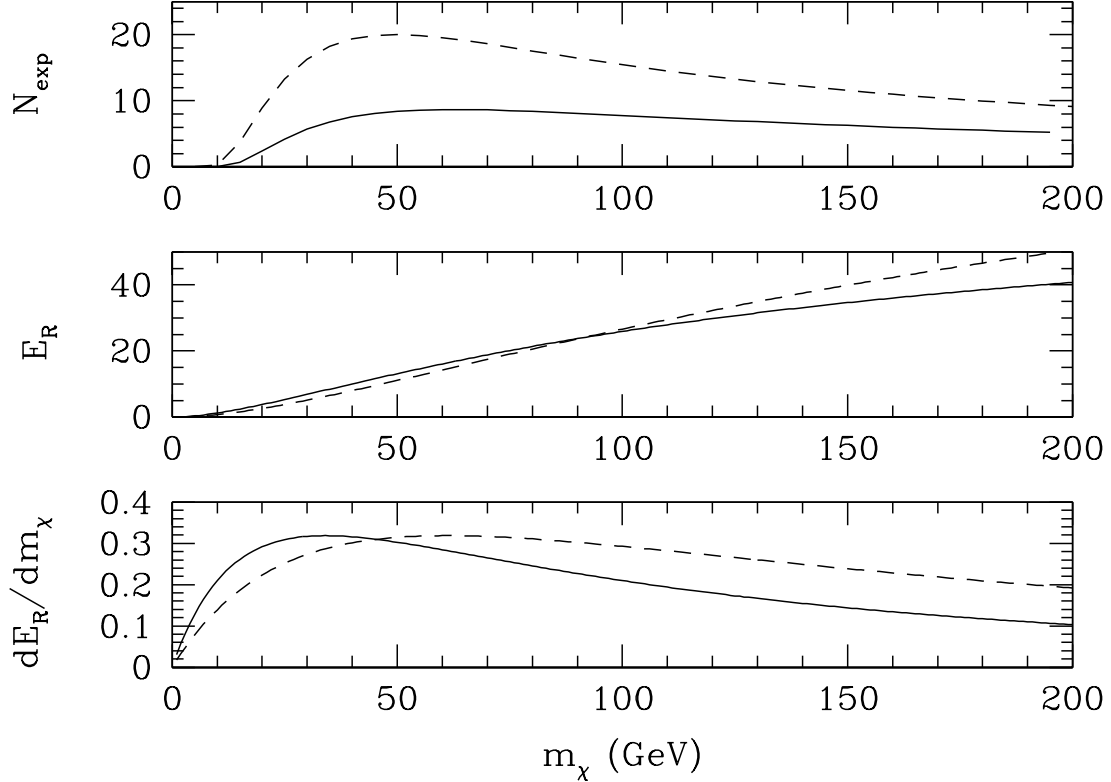


Figure 1. From top panel to bottom: the expected number of events, N_{exp} , for a $\mathcal{E} = 3 \times 10^3$ kg day exposure (with $\sigma_p = 10^{-8}$ pb), the characteristic energy scale, E_R , and the variation of the characteristic energy scale with mass, dE_R/dm_χ , as a function of WIMP mass for a Ge detector (solid line) and a Xe detector (dashed). For N_{exp} the energy thresholds of the current CDMS II [21] and Xenon10 [22] experiments have been used: $E_{\text{th}} = 10$ keV and 4.5 keV for Ge and Xe respectively.

The characteristic energy, E_R , depends on the WIMP mass, m_χ , and the mass of the target nuclei, m_A . For WIMPs which are light compared with the target nuclei, $m_\chi \ll m_A$, $E_R \propto m_\chi^2/m_A$, while for heavy WIMPs, $m_\chi \gg m_A$, $E_R \sim \text{const}$. In words, for light WIMPs the energy spectrum is strongly dependent on the WIMP mass while for heavy WIMPs the dependence on the WIMP mass is far weaker. Consequently it will be easier to measure the mass of light (compared with the target nuclei) than heavy WIMPs. Since the experiments which currently have the greatest sensitivity are composed of Ge and Xe (CDMS II [21] and Xenon10 [22] respectively) we focus on these targets. Fig. 1 shows the dependence of the characteristic energy, E_R , and dE_R/dm_χ on the WIMP mass for Ge and Xe. For $m_\chi < (>) \sim 50$ GeV E_R varies more strongly with m_χ for Ge (Xe), reflecting the asymptotic WIMP mass dependences of the expression for E_R . This suggests that light (heavy) target nuclei will be better suited to determining the mass of light (heavy) WIMPs (see however Sec. 3.2). The detector energy threshold will also come into play, in particular for small exposures, as the expected number of

events depends on the energy threshold. The expected number of events, N_{exp} , for an exposure of $\mathcal{E} = 3 \times 10^3$ kg day is also shown in fig. 1 as a function of WIMP mass for Ge and Xe detectors with $E_{\text{th}} = 10$ keV [21, 13] and 4.5 keV [22] respectively. With these thresholds N_{exp} is larger (by a factor of order ~ 2 for $m_\chi \approx 50$ GeV) for Xe than for Ge. This indicates that the relative capabilities of detectors to determine the WIMP mass will depend not only on the WIMP and target masses, but also on their energy thresholds.

2.2. Monte Carlo simulations

We use Monte Carlo simulations to examine, for a range of detector configurations and input WIMP masses, how well the WIMP mass could be determined from the energies of observed WIMP nuclear recoil events.

We estimate the WIMP mass and cross-section by maximizing the extended likelihood function (which takes into account the fact that the number of events observed in a given experiment is not fixed), e.g. Ref. [23]:

$$L = \frac{\lambda^{N_{\text{expt}}} \exp(-\lambda)}{N_{\text{expt}}!} \prod_{i=1}^{N_{\text{expt}}} f(E_i). \quad (9)$$

Here N_{expt} is the number of events observed, E_i ($i = 1, \dots, N_{\text{expt}}$) are the energies of the events observed, $f(E)$ is the normalized differential event rate and $\lambda = \mathcal{E} \int_{E_{\text{th}}}^{\infty} (dR/dE) dE$ is the mean number of events where \mathcal{E} is the detector exposure (which has dimensions of mass times time) and E_{th} is the threshold energy. We calculate the probability distribution of the maximum likelihood estimators of the WIMP mass and cross-section, for each detector configuration and input WIMP mass, by simulating 10^4 experiments. We first calculate the expected number of events, λ_{in} , from the input energy spectrum. The actual number of events for a given experiment, N_{expt} , is drawn from a Poisson distribution with mean λ_{in} . We Monte Carlo generate N_{expt} events from the input energy spectrum, from which the maximum likelihood mass and cross-section for that experiment are calculated. Finally we find the (two-sided) 68% and 95% confidence limits on the WIMP mass from the maximum likelihood masses.

3. Results

In Sec. 3.1 we investigate the mass limits for a SuperCDMS like Ge detector [13] and their dependence on the detector energy threshold, maximum energy and exposure, and the WIMP cross-section. In Sec. 3.2 we compare the Ge mass limits with those for a Xe detector, before examining the effects of uncertainties in the local circular speed and non-negligible background in Secs. 3.3 and 3.4 respectively.

3.1. Germanium

We begin, as in paper I [10], by looking at a SuperCDMS like detector [13], composed of Ge with a nuclear recoil energy threshold of $E_{\text{th}} = 10$ keV. We assume that the

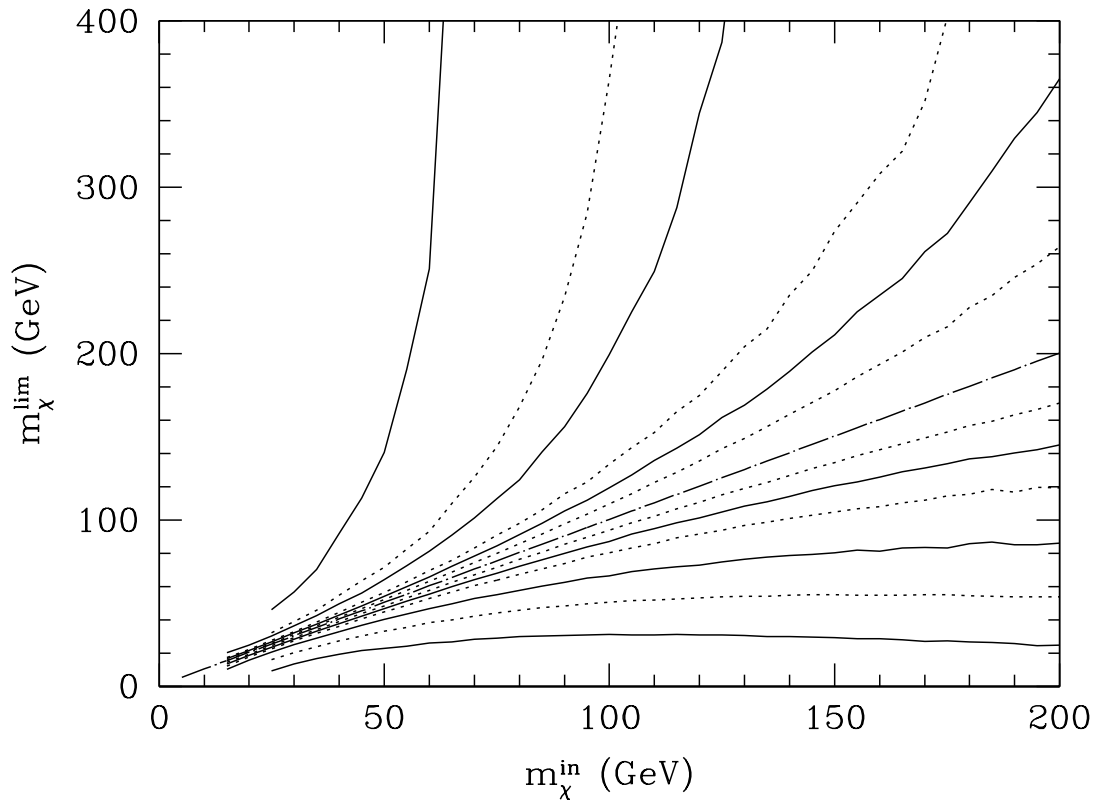


Figure 2. Limits on the WIMP mass, m_χ^{lim} , as a function of the input WIMP mass, m_χ^{in} , for the benchmark Ge detector ($E_{\text{th}} = 10$ keV, perfect energy resolution, no upper limit on energy of events detected and zero background) for exposures $\mathcal{E} = 3 \times 10^3, 3 \times 10^4$ and 3×10^5 kg day and input cross-section $\sigma_p = 10^{-8}$ pb. The dot-dashed line is the input mass and the solid (dotted) lines are the 95% (68%) confidence limits.

background event rate is negligible, as is expected for this experiment located at SNOLab [13], and that the energy resolution is perfect ‡. For simplicity we assume that the nuclear recoil detection efficiency is independent of energy. The energy dependence of the efficiency of the current CDMS II experiment is relatively small (it increases from ~ 0.22 at $E = E_{\text{th}} = 10$ keV to ~ 0.30 at $E = 15$ keV and then remains roughly constant). For further discussion of these assumptions see Ref. [10].

We consider fiducial efficiency weighted exposures § $\mathcal{E} = 3 \times 10^3, 3 \times 10^4$ and 3×10^5 kg day which correspond, roughly, to a detector with mass equal to that of the 3 proposed phases of SuperCDMS taking data for a year with a $\sim 50\%$ detection efficiency ||.

‡ Gaussian energy resolution, with full width at half maximum of order 1 keV [13], does not affect the WIMP parameters extracted from the energy spectrum [10].

§ For brevity we subsequently refer to this as simply the exposure.

|| The 50% detection efficiency was chosen based on Ref [24]. The more recent CDMS II analysis [21]

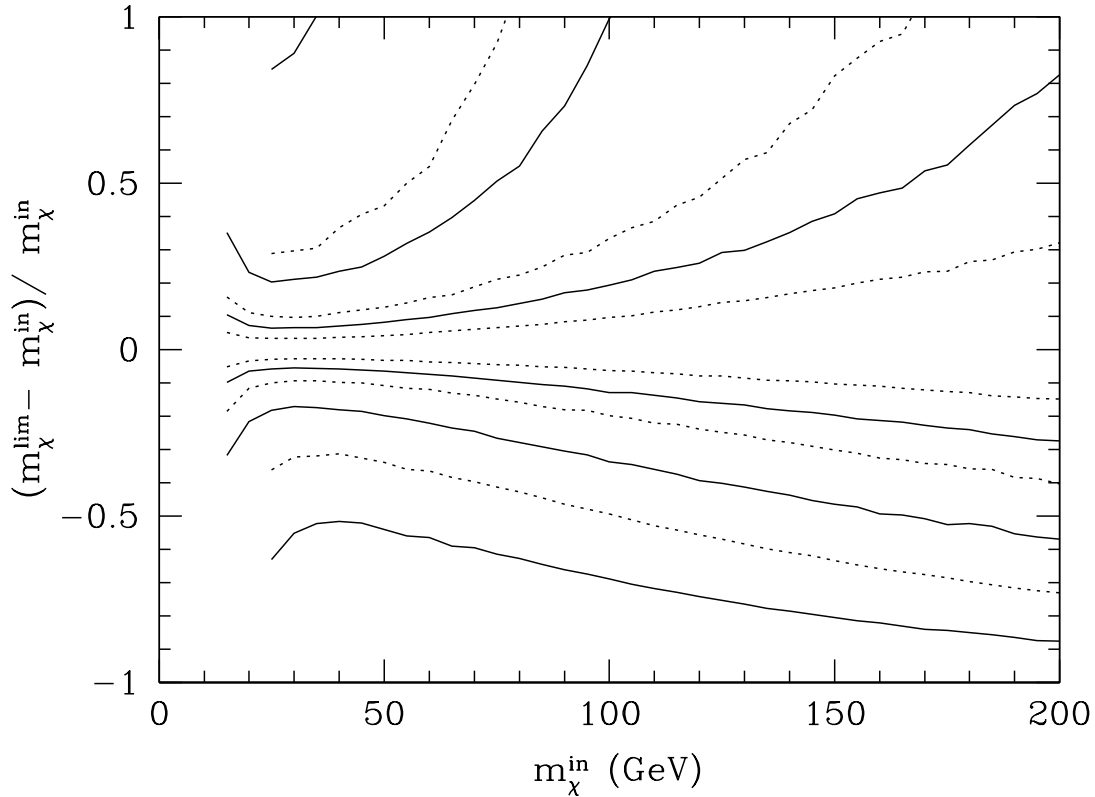


Figure 3. As fig. 2, but with the fractional deviation of the WIMP mass limits from the input mass, $(m_\chi^{\text{lim}} - m_\chi^{\text{in}})/m_\chi^{\text{in}}$, plotted.

We use fiducial values for the detector energy threshold and WIMP-proton cross-section of $E_{\text{th}} = 10 \text{ keV}$ and $\sigma_p = 10^{-8} \text{ pb}$ but later, in Secs. 3.1.1 and 3.1.4 respectively, consider a range of values for these parameters. Note that this fiducial cross-section is, given the recent limits from the CDMS II [21] and Xenon10 [22] experiments, an order of magnitude smaller than that used in Paper I [10]. We use the standard values for the local circular speed and WIMP density, $v_c = 220 \text{ km s}^{-1}$ and $\rho_\chi = 0.3 \text{ GeV cm}^{-3}$ respectively. We examine the effect of uncertainties in the local circular speed in Sec. 3.3. The local WIMP density only affects the amplitude, and not the shape, of the energy spectrum. Therefore it only affects the WIMP mass determination indirectly, through the number of events detected. We note that the limits from our idealized simulated detector are likely to be better than those achievable in reality by a real detector.

In fig. 2 we plot the 68% and 95% confidence limits on the WIMP mass, m_χ^{lim} , for the fiducial detector configuration as a function of the input WIMP mass, m_χ^{in} . Here, and throughout, the limits terminate when there is a $> 5\%$ probability that an experiment will detect no events. Fig. 3 uses the same data, but shows the fractional limits on has a lower nuclear recoil acceptance, $\sim 30\%$.

Table 1. Dependence of the 95% fractional confidence limits on the WIMP mass, $(m_\chi^{\text{lim}} - m_\chi)/m_\chi$, on the energy threshold, E_{th} , for the benchmark Ge detector, for input WIMP masses $m_\chi^{\text{in}} = 50, 100$ and 200 GeV and exposure $\mathcal{E} = 3 \times 10^5$ kg day.

E_{th} (keV)	m_χ^{in} (GeV)		
	50	100	200
0	-0.064 , +0.043	-0.12 , +0.14	-0.25 , +0.63
10	-0.082 , +0.057	-0.13 , +0.18	-0.27 , +0.81
20	-0.11 , +0.073	-0.16 , +0.22	-0.31 , +1.1

the WIMP mass, $(m_\chi^{\text{lim}} - m_\chi^{\text{in}})/m_\chi^{\text{in}}$. With exposures of $\mathcal{E} = 3 \times 10^4$ and 3×10^5 kg day it would be possible, with this detector configuration, to measure the mass of a light [$m_\chi \sim \mathcal{O}(50 \text{ GeV})$] WIMP with an accuracy of roughly 25% and 10% respectively. These numbers, and the upper limits in particular, increase with increasing WIMP mass, and for heavy WIMPs ($m_\chi \gg 100 \text{ GeV}$) even with a large exposure it will only be possible to place a lower limit on the mass. For very light WIMPs, $m_\chi < \mathcal{O}(20 \text{ GeV})$, the number of events above the detector energy threshold would be too small to allow the mass to be measured accurately.

3.1.1. Energy threshold We now examine the effects of varying the energy threshold, E_{th} (for the fiducial detector configuration and WIMP properties described above). Table 1 contains the 95% confidence limits on the fractional deviation of the WIMP mass from the input WIMP mass for input WIMP masses of $m_\chi^{\text{in}} = 50, 100$ and 200 GeV, energy thresholds $E_{\text{th}} = 0, 10$ and 20 keV and an exposure of $\mathcal{E} = 3 \times 10^5$ kg day.

As the energy threshold is increased the expected number of events decreases. The smaller range of recoil energies also reduces the accuracy with which the characteristic scale of the energy spectrum, E_{R} , and hence the WIMP mass can be determined. The effect of varying E_{th} is smallest for intermediate WIMP masses; for $m_\chi = 50$ GeV (and light WIMPs in general) the small E_{R} means that expected number of events decreases rapidly as the energy threshold is increased, while for $m_\chi = 200$ GeV (and heavy WIMPs in general) the large E_{R} , and flatter energy spectrum, means that the smaller range of recoil energies reduces the accuracy with which E_{R} can be measured.

3.1.2. Maximum energy We have previously assumed that recoil events of all energies above the threshold energy can be detected. In real experiments there will be a maximum energy, E_{max} , above which recoils are not detected/analysed. For instance for CDMS II [21] $E_{\text{max}} = 100$ keV. Fig. 4 compares the fractional mass limits for $E_{\text{max}} = 100$ keV with those found previously assuming no upper limit. The difference is very small for light WIMPs [$m_\chi < \mathcal{O}(50 \text{ GeV})$] increasing with increasing m_χ to $\mathcal{O}(10\%)$ for $m_\chi \sim \mathcal{O}(200 \text{ GeV})$ and $\mathcal{E} = 3 \times 10^5$ kg day. This reflects the fact that for light WIMPs the differential event rate above E_{max} is essentially negligible, however this

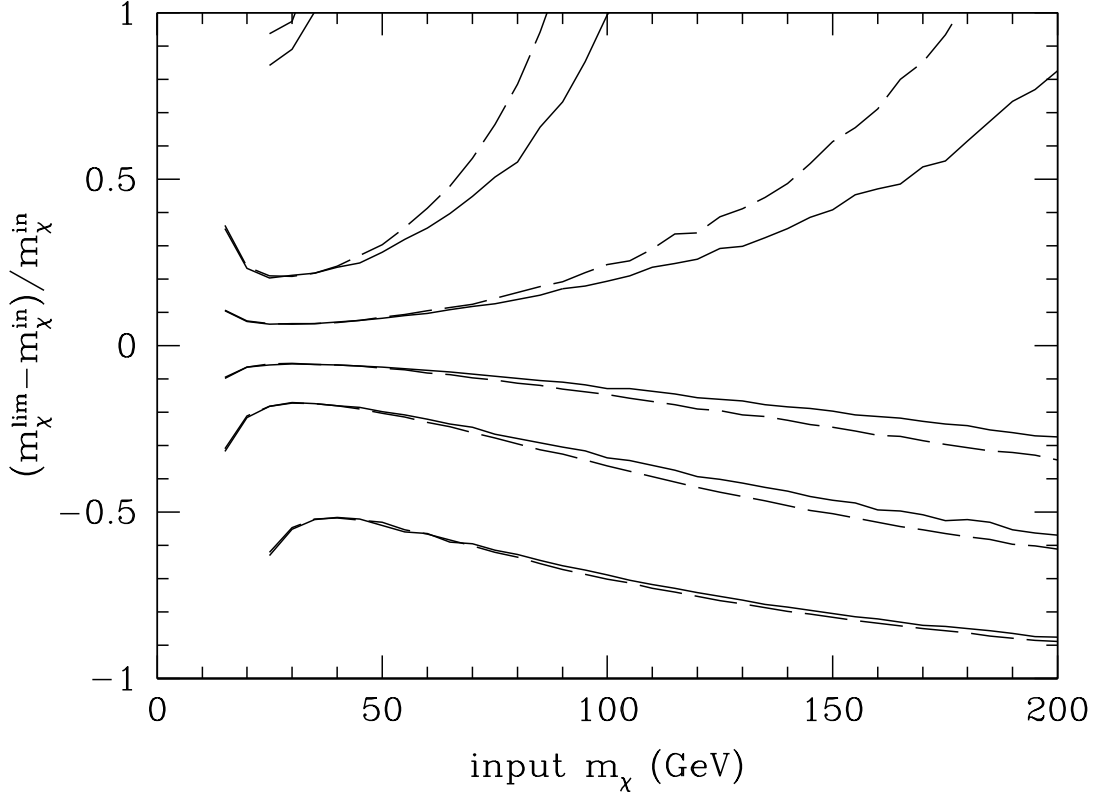


Figure 4. Fractional mass limits as a function of input mass for the fiducial detector configuration, with no limit on the energy of recoils which can be detected, (solid lines as before) and for a maximum energy $E_{\max} = 100$ GeV (long dashed). For clarity only the 95% confidence limits are displayed in this figure.

is not the case for heavier WIMPs and finite E_{\max} reduces the accuracy with which the characteristic energy scale of the spectrum can be measured.

3.1.3. Exposure Fig. 5 shows the fractional limits on the WIMP mass as a function of the exposure, \mathcal{E} , for input WIMP masses of $m_{\chi}^{\text{in}} = 50, 100$ and 200 GeV, for the fiducial detector and $\sigma_{\text{p}} = 10^{-8}$ pb. As the exposure is increased the mass limits (and in particular the 95% upper confidence limit) improve, initially rapidly and then more slowly (reflecting the fact that the expected number of events is directly proportional to the exposure). An accuracy of $\sim \pm 10\%$ in the determination of the WIMP mass can be achieved with an exposure $\mathcal{E} = 10^5$ (10^6) kg day for $m_{\chi}^{\text{in}} = 50$ (100) GeV. For $m_{\chi}^{\text{in}} = 200$ GeV even $\mathcal{E} = 10^6$ kg day would not be sufficient to achieve $\mathcal{O}(10\%)$ precision.

3.1.4. Cross-section The expected number of events is directly proportional to both the cross-section and exposure. Varying the cross-section is therefore very similar to varying the exposure (and hence we do not display a plot of the limits for varying σ_{p}).

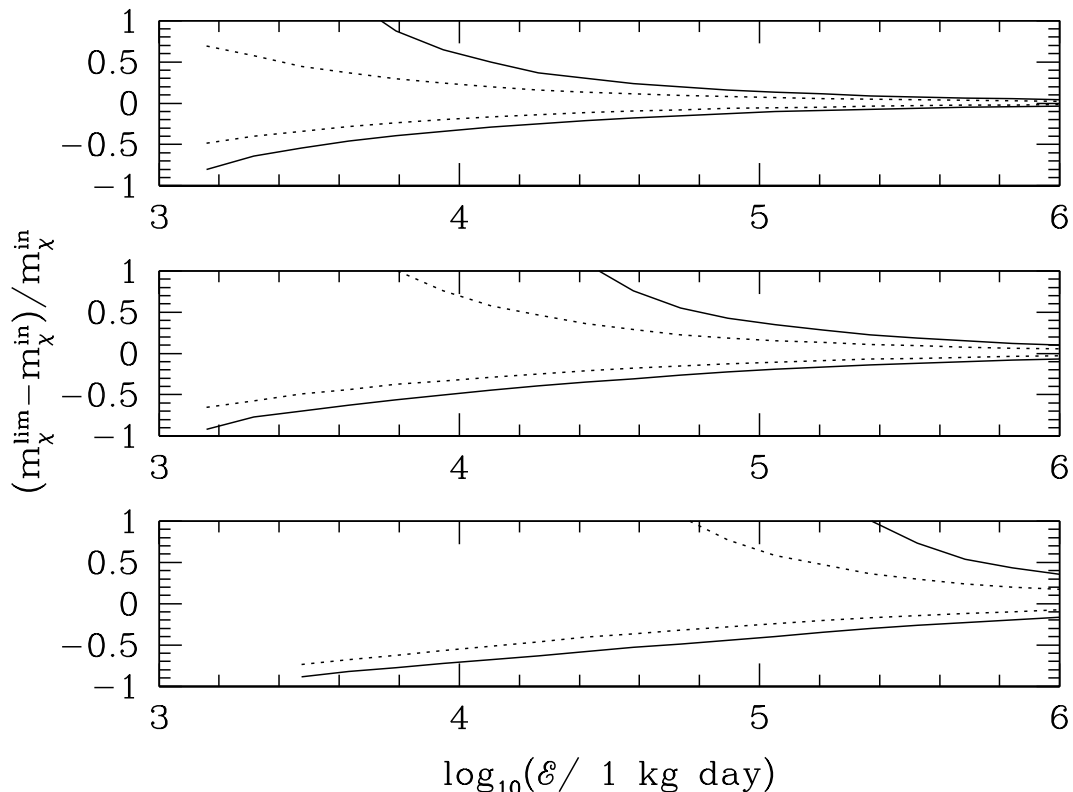


Figure 5. Fractional mass limits as a function of exposure, \mathcal{E} , for the benchmark Ge detector and $\sigma_p = 10^{-8}$ pb, for, from top to bottom, $m_\chi^{\text{in}} = 50, 100$ and 200 GeV.

Unsurprisingly the accuracy with which it will be possible to determine the WIMP mass depends sensitively on the underlying cross-section. For instance if $\sigma_p = 10^{-9}$ pb, with an exposure of $\mathcal{E} = 3 \times 10^5$ kg day it will be possible to measure the mass with an accuracy of $\sim \pm 20\%$ ($^{+100\%}_{-30\%}$) for $m_\chi^{\text{in}} = 50$ (100) GeV. If $\sigma_p = 10^{-10}$ pb, even for $m_\chi^{\text{in}} = 50$ GeV with an exposure of $\mathcal{E} = 3 \times 10^5$ kg day it will only be possible to determine the WIMP mass to within a factor of a few and for more massive WIMPs it will only be possible to place a lower limit on the mass.

3.2. Xenon

We now examine the dependence of the mass limits on the detector target material. In fig. 6 we compare the fractional limits for the fiducial (Super-CDMS [13] like) detector with $E_{\text{th}} = 10$ keV with those from a Xe detector with $E_{\text{th}} = 4.5$ keV (c.f. Xenon10 [22]) and 10 keV. The difference in the mass limits for the different detector configurations is largest for small exposures, where the number of events observed is small. For light WIMPs, as found in Sec. 3.1.1, the energy threshold is important, with the Xe detector with $E_{\text{th}} = 4.5$ keV doing significantly better than both the fiducial Ge detector and also

the Xe detector with $E_{\text{th}} = 10 \text{ keV}$. For heavier WIMPs, $m_\chi > 100 \text{ GeV}$, in contrast to the naive expectation from the m_χ dependence of E_{R} (see Sec. 2.1), the Ge detector produces slightly better limits than the Xe detector with $E_{\text{th}} = 4.5 \text{ keV}$. This is because of the rapid decrease of the Xe form factor with increasing energy/momentum transfer. In fig. 7 we compare, for a Ge detector with $E_{\text{th}} = 10 \text{ keV}$ and a Xe detector with $E_{\text{th}} = 4.5 \text{ keV}$, the mass limits we found before with those which would be obtained if the form factor were equal to unity for all energies, $F(E) = 1$. Without the form factor the mass limits are substantially tighter for both Ge and Xe. This is because the event rate, in particular at large energies, is increased. The improvement in the accuracy of the determination of the characteristic energy, E_{R} , and hence m_χ , is greater than if the exposure were simply increased so as to increase the expected number of events. For instance for Xe, $m_\chi = 200 \text{ GeV}$ and $\mathcal{E} = 3 \times 10^5 \text{ kg day}$ without the form factor the one- σ error on the WIMP mass is $\sim 3 \text{ GeV}$, while with the form factor included if the exposure is increased so as to give the same expected number of events the one- σ error is $\sim 20 \text{ GeV}$. This is because the greater relative abundance of large energy recoils allows E_{R} to be determined more accurately. With the form factor set to unity the mass limits for large WIMP masses are significantly better for Xe than for Ge, as naively expected from the WIMP mass dependence of E_{R} . However for any real detector the rapid decrease of the Xe form factor with increasing energy/momentum transfer means that, contrary to naive expectations, the mass of heavy WIMPs can not be measured more accurately with Xe than with Ge (assuming similar threshold energies). This conclusion, see also recent discussion by Drees and Shan [11], should also hold for any other heavy target.

3.3. Varying input circular speed, v_c

Up until now we have assumed that the local circular speed, v_c , is known and equal to its standard value of 220 km s^{-1} . There is in fact an uncertainty in v_c of order $\pm 20 \text{ km s}^{-1}$ [15] and since E_{R} depends on both m_χ and v_c there is a degeneracy between m_χ and v_c [10]. Physically, the kinetic energies of the incoming WIMPs depend on their mass and velocities. For larger (smaller) v_c the incoming WIMPs have larger (smaller) mean kinetic energies than assumed, resulting in larger (smaller) maximum likelihood mass values. This can be made more quantitative by differentiating the expression for the characteristic energy E_{R} , eq. (8):

$$\frac{\Delta m_\chi}{m_\chi} = -[1 + (m_\chi/m_A)] \frac{\Delta v_c}{v_c}. \quad (10)$$

For an input WIMP mass of $m_\chi^{\text{in}} = 100 \text{ GeV}$ and a 20 km s^{-1} uncertainty in v_c , this gives a $\sim 20 \text{ GeV}$ shift in the value of the WIMP mass determined.

In fig. 8 we plot the fractional mass limits for input circular speeds $v_c^{\text{in}} = 200, 220$ and 240 km s^{-1} for $\mathcal{E} = 3 \times 10^5 \text{ kg day}$. We carry out the likelihood analysis twice, once with v_c fixed at 220 km s^{-1} and once with v_c as an additional variable parameter. As discussed in Sec. 2.1 in this section we use the fitting function, eq. (6), for both the

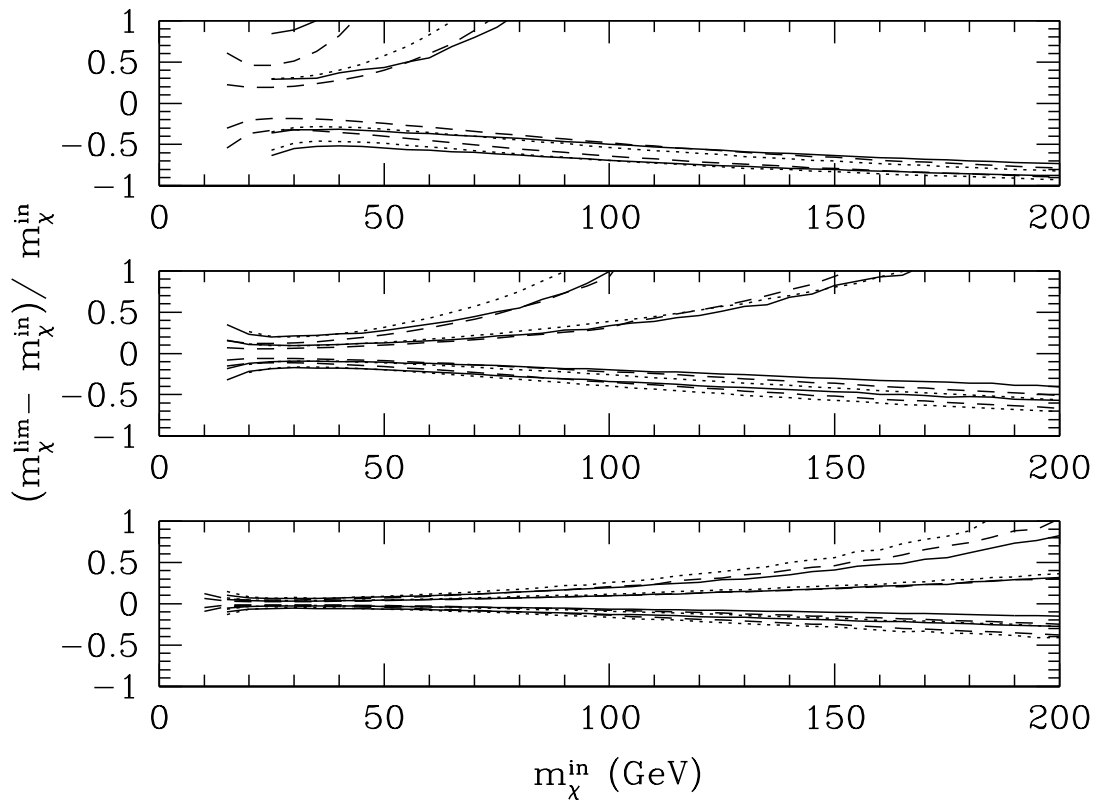


Figure 6. Fractional mass limits for the fiducial Ge detector with $E_{\text{th}} = 10$ keV (solid lines for both 68% and 95% confidence limits) and for a Xe detector with $E_{\text{th}} = 4.5$ and 10 keV (dashed and dotted lines respectively) for (from top to bottom) $\mathcal{E} = 3 \times 10^3, 3 \times 10^4$ and 3×10^5 kg day.

input energy spectrum and the likelihood analysis as it is not computationally feasible to carry out the full calculation of the energy spectrum for each value of v_c considered during the likelihood analysis.

When the underlying value of v_c^{in} is different from the (fixed) value used in the likelihood analysis there is, as expected, a significant systematic error in the determination of the WIMP mass. For deviations of ± 20 km s $^{-1}$ in the underlying value of v_c this systematic error increases with increasing m_χ^{in} from $\sim 10\%$ for small m_χ^{in} to $\sim 40\%$ for $m_\chi \approx 200$ GeV. The limits are however asymmetric, with the systematic error in the upper limits being substantially larger for $v_c^{\text{in}} = 200$ km s $^{-1}$. Allowing the value of v_c to vary in the likelihood analysis substantially reduces the error, but there still appears to be a small systematic shift in the mass limits.

3.4. Backgrounds

While future experiments aim to have negligible backgrounds (e.g. Ref. [13]), non-negligible neutron backgrounds would lead to errors in the determination of the WIMP

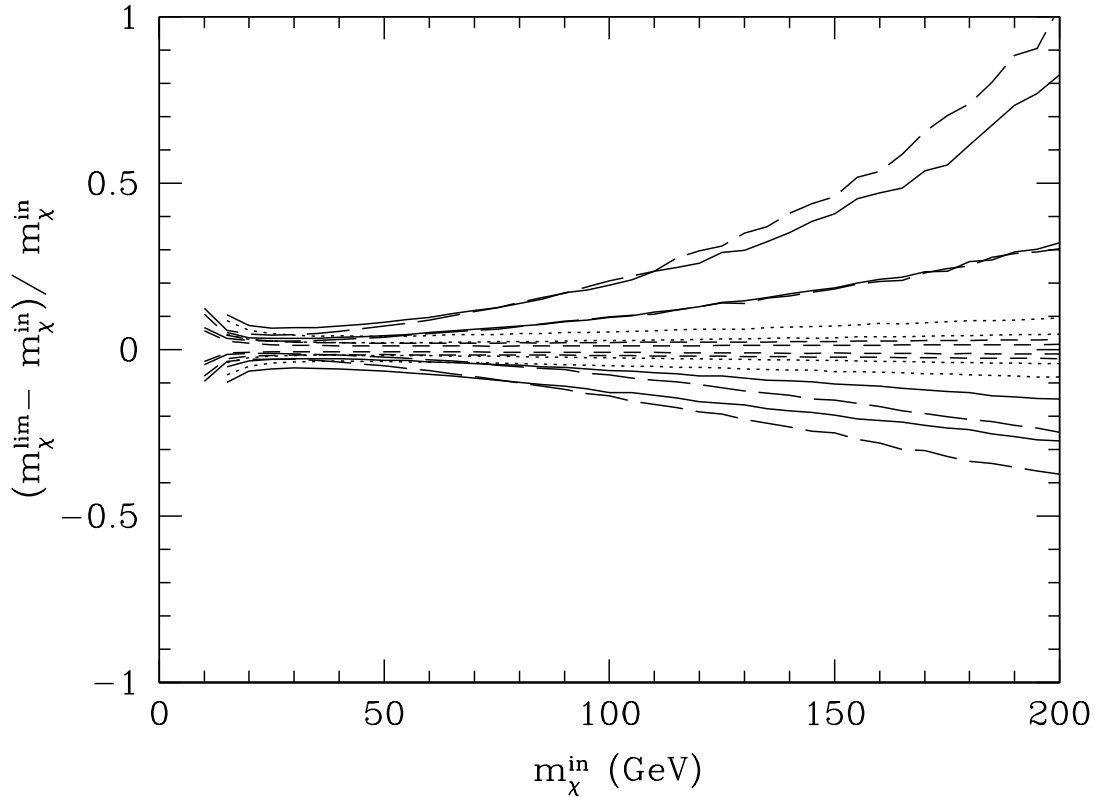


Figure 7. A comparison of the fractional mass limits obtained, for Ge and Xe with an exposure $\mathcal{E} = 3 \times 10^5$ kg day, with and without the form factor. The solid and long dashed lines are for the fiducial Ge detector with $E_{\text{th}} = 10$ keV and for a Xe detector with $E_{\text{th}} = 4.5$ keV respectively, as in the bottom panel of Fig. 6. The dotted and short dashed lines are for the same Ge and Xe detectors, with the form factor artificially set to unity, $F(E) = 1$.

mass. The size of the errors will depend on the amplitude and shape of the background spectrum. In particular if the background spectrum is exponential it can closely mimic the shape of a WIMP recoil spectrum (see fig. 9).

Motivated by simulations of the neutron background in various dark matter detectors [25] we consider two forms for the background

- (i) A flat background energy spectrum from $E_{\text{th}} = 10$ keV to $E_{\text{max}} = 100$ keV ¶ , parametrised by the total background rate, b_r , per tonne year.
- (ii) A exponential energy spectrum from $E_{\text{th}} = 10$ keV to $E_{\text{max}} = 100$ keV, parametrised by the total background rate, b_r , per tonne year, and the characteristic background energy scale, E_b :

$$\left(\frac{dR}{dE}\right)_{\text{back}} = \left(\frac{dR}{dE}\right)_{E=0} \exp[-(E/E_b)], \quad (11)$$

¶ In this section we assume that only recoils up to E_{max} are detected.

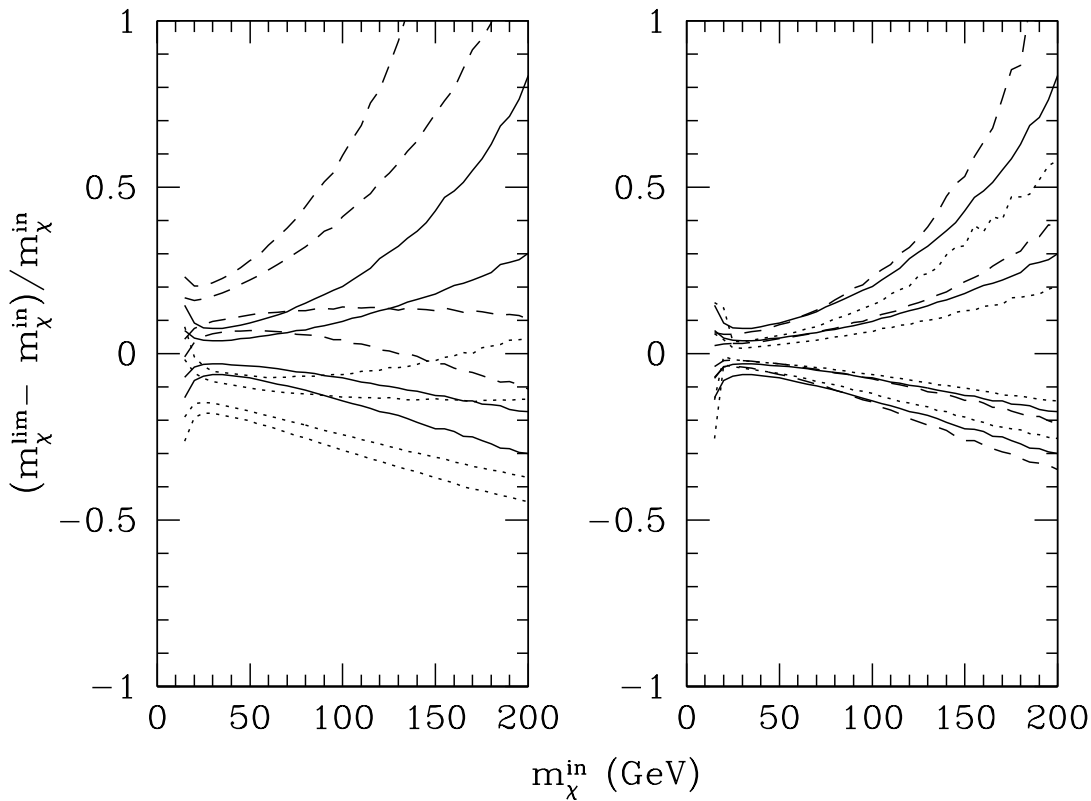


Figure 8. Fractional mass limits for the fiducial Ge detector and $\mathcal{E} = 3 \times 10^5$ kg day for varying circular speed, v_c . In the left panel v_c is fixed as 220 km s^{-1} in the likelihood analysis while in the right panel v_c is allowed to vary in the likelihood analysis (i.e. it is an additional fitting parameter). Solid, dotted and dashed lines are for $v_c^{\text{in}} = 220, 200$ and 240 km s^{-1} respectively.

where

$$b_r = \int_{E_{\text{th}}}^{E_{\text{max}}} \left(\frac{dR}{dE} \right)_{\text{back}} . \quad (12)$$

The limits on the WIMP mass for an exposure of $\mathcal{E} = 3 \times 10^5$ kg day and $\sigma_p = 10^{-8}$ pb in the presence of a flat background with $b_r = 10$ and $100 \text{ tonne}^{-1} \text{ year}^{-1}$ + are displayed in fig. 10. We carry out the likelihood analysis of the WIMP parameters twice, firstly neglecting the background and then including the background rate as an additional parameter. Neglecting the background leads to a systematic over-estimate of the WIMP mass, since the flat background increases the event rate at large E relative to that at small E , so that the best fit energy spectrum has larger E_R , or equivalently larger m_χ . Including the background rate in the likelihood analysis avoids the systematic error but, inevitably, leads to larger statistical error in the WIMP mass limits. The fractional errors are smallest for $m_\chi \sim \mathcal{O}(50 \text{ GeV})$ and increase for smaller and larger

+ Note that the backgrounds in real experiments are not expected to be this large.

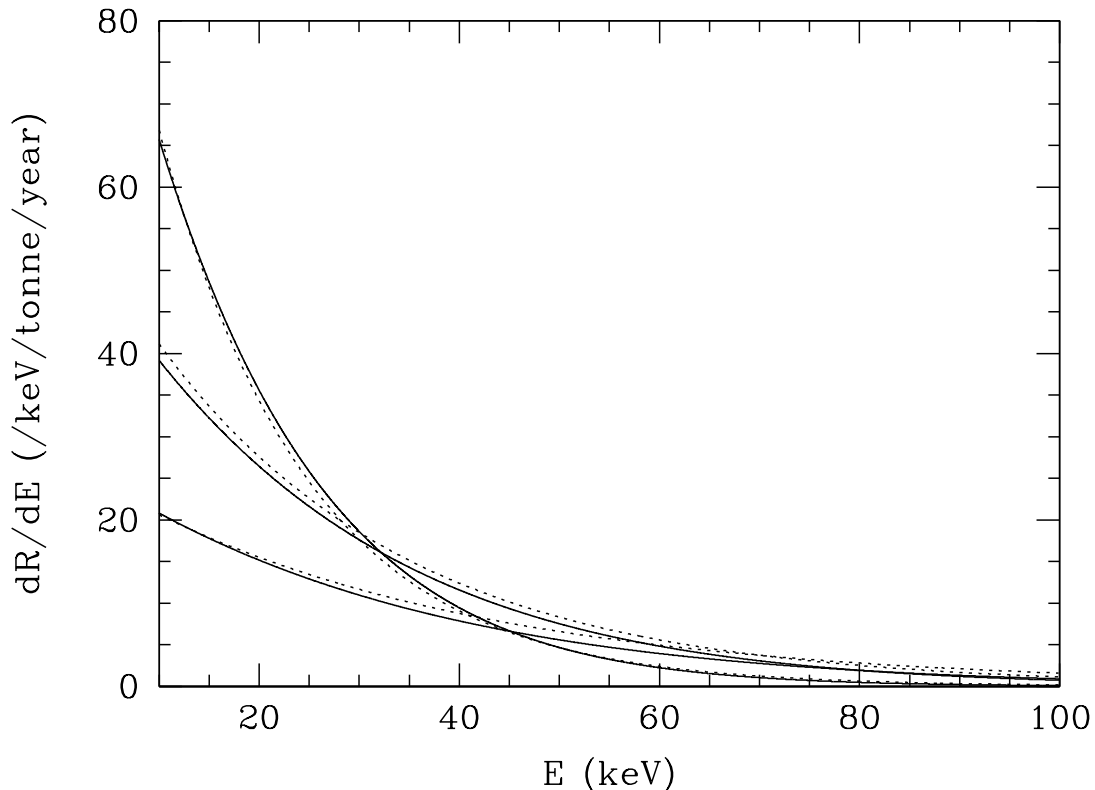


Figure 9. Solid lines are the differential energy spectra including the form factor, dR/dE , for (from top to bottom at $E = 0$ keV) WIMPs with $m_\chi = 50, 100$ and 200 GeV (solid lines). The dotted lines are exponential background spectra with (from top to bottom) $b_r = 1000 \text{ tonne}^{-1}\text{year}^{-1}$ & $E_b = 15$ keV, $b_r = 1000 \text{ tonne}^{-1}\text{year}^{-1}$ & $E_b = 25$ keV and $b_r = 670 \text{ tonne}^{-1}\text{year}^{-1}$ & $E_b = 35$ keV (dotted lines). The parameters of the exponential background spectra have been chosen to demonstrate that, even when the form factor is included, the WIMP recoil spectra are close to exponential and could, in principle, be mimicked by an exponential background.

WIMP masses. This is because for small WIMP masses the background event rate is larger compared with the WIMP event rate, while for large WIMP masses the WIMP energy spectrum (exponential with large characteristic energy scale) is closer in shape to the flat background spectrum. The systematic (background not included in analysis) and additional statistical (background rate included) errors are both at least 10% for $b_r = 10 \text{ tonne}^{-1} \text{ year}^{-1}$. For $b_r = 100 \text{ tonne}^{-1} \text{ year}^{-1}$ the minimum systematic error (for $m_\chi \sim 50$ GeV) is $\sim 30\%$, the shift in the lower limits when the background is included in the likelihood analysis is not much larger than for $b_r = 10 \text{ tonne}^{-1} \text{ year}^{-1}$, however the upper limits are increased significantly.

The limits on the WIMP mass for an exposure of $\mathcal{E} = 3 \times 10^5 \text{ kg day}$ and $\sigma_p = 10^{-8} \text{ pb}$ in the presence of a background with an exponential energy spectrum with $E_b = 20$ keV are displayed in fig. 11. The exponential background spectrum with

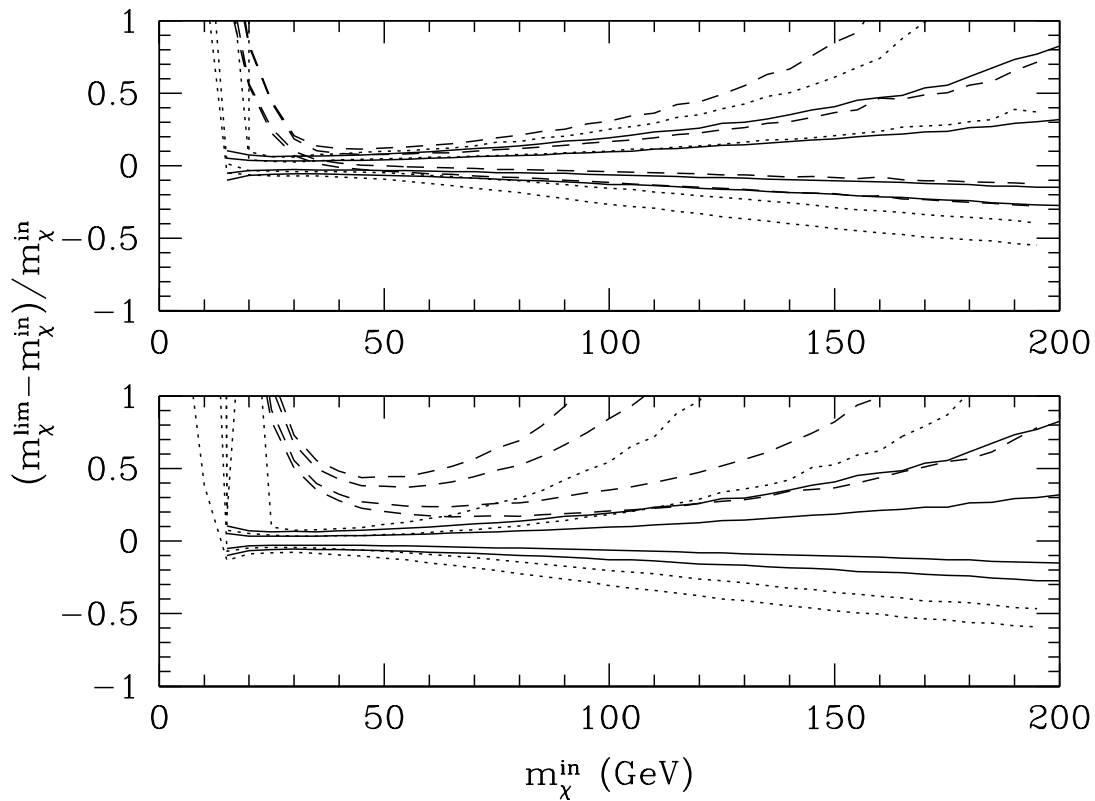


Figure 10. Fractional mass limits in the presence of a background with a flat energy spectrum and total rate $b_r = 10$ and $100 \text{ tonne}^{-1} \text{ year}^{-1}$ (top and bottom panels respectively). The dashed (dotted) lines are for when the background event rate is not (is) included in the likelihood analysis. The solid lines are the confidence limits for zero background. The fiducial Ge detector configuration with $E_{\text{max}} = 100 \text{ keV}$, $\mathcal{E} = 3 \times 10^5 \text{ kg day}$ and $\sigma_p = 10^{-8} \text{ pb}$ is used.

$E_b = 20 \text{ keV}$ is similar to the WIMP spectrum with $m_\chi \sim 70 \text{ GeV}$. Therefore if the background is neglected in the likelihood analysis, for smaller (larger) input WIMP masses the WIMP mass is systematically over(under)-estimated. For the exponential background when the background rate, b_r , and characteristic energy, E_b , are included in the likelihood analysis there are still large deviations from the zero background limits, this is because the WIMP and background spectra can have extremely similar shapes and can be degenerate. The fluctuations in the limits with varying m_χ^{in} reflect the errors resulting from this degeneracy rather than a real underlying trend.

In summary the implications of non-negligible backgrounds for the determination of the WIMP mass depend strongly on the shape of the background spectra (as well as, obviously, its amplitude). A flat background spectrum will lead to a systematic error in the WIMP mass for light WIMPs, which can be avoided, at the cost of larger statistical error, by fitting for the background event rate. For heavier WIMPs the flat

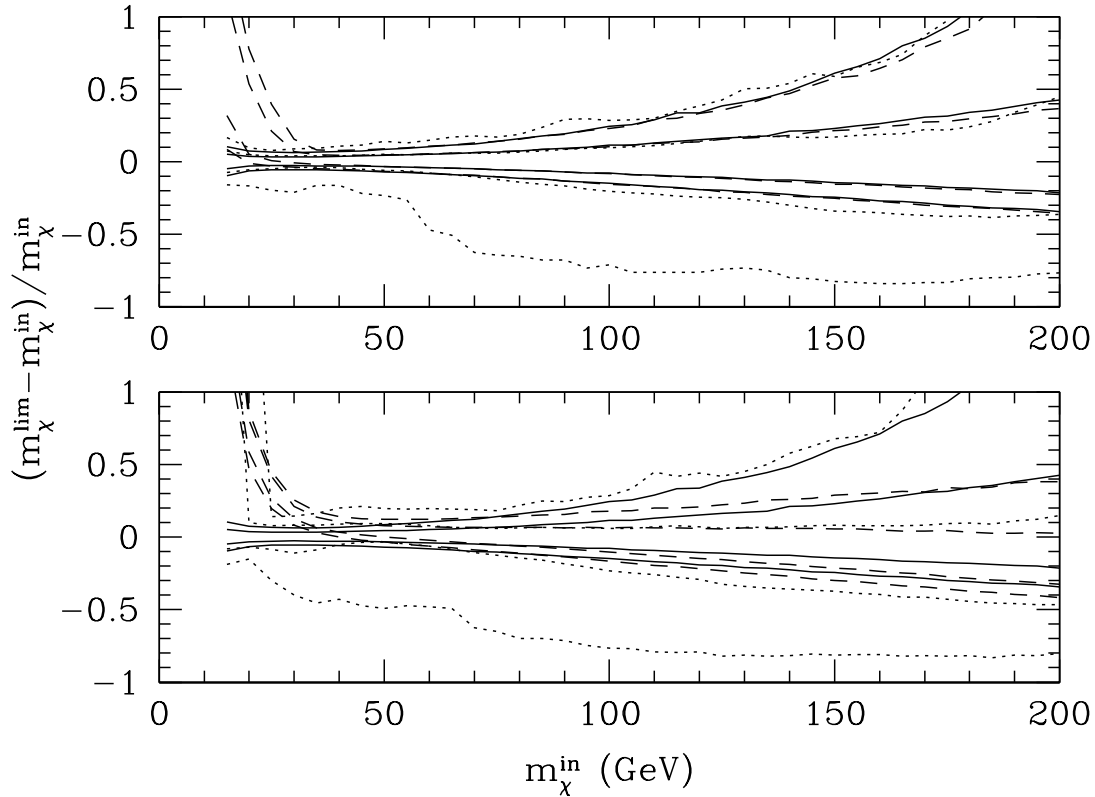


Figure 11. As fig. 10 for an exponential background energy spectrum with $E_b = 20$ keV.

background is similar in shape to the WIMP spectrum and it is hence more difficult to separate the WIMP and background spectra and accurately measure the WIMP mass. An exponential background spectrum is similar in shape to the WIMP spectrum and would inevitably (even when the background parameters are including in the likelihood analysis) lead to increased errors in the determination of the WIMP mass.

With a single detector it will be difficult to disentangle a WIMP signal (and the WIMP mass) from background if the background spectrum has a similar shape to the WIMP spectrum (i.e. exponential background, or flat background with a heavy WIMP). Multiple targets (for instance Ge and Si as used by CDMS II [21]) would help due to the dependence of the WIMP spectrum on the mass of the target nuclei. See ref. [26] for Monte Carlo simulations using CaWO_4 and ZnWO_4 . Detectors composed of very different targets (e.g. Ge and Xe) would likely have different background spectra however.

4. Summary

We have studied how the accuracy with which the WIMP mass could be determined by a single direct detection experiment depends on the detector configuration and the WIMP properties. Specifically, we investigated the effects of varying the underlying WIMP mass and cross-section, the detector target nucleus, exposure, energy threshold and maximum energy, the local circular speed and the background event rate and spectrum.

The accuracy of the mass limits is most strongly dependent on the underlying WIMP mass and the number of events detected. For light WIMPs (mass significantly less than that of the target nuclei) small variations in the WIMP mass lead to significant changes in the energy spectrum. Conversely for heavy WIMPs the energy spectrum depends only weakly on the WIMP mass. Consequently it will be far easier to measure the WIMP mass if it is light than if it is heavy. The number of events detected is directly proportional to both the exposure and the cross-section, therefore these quantities have the greatest bearing on the accuracy of the WIMP mass determination. For our baseline, SuperCDMS [13] like, Ge detector with negligible background and energy threshold $E_{\text{th}} = 10$ keV for a WIMP-proton cross-section of $\sigma_p = 10^{-8}$ pb, a factor of a few below the current exclusion limits from the CDMS II [21] and Xenon10 [22] collaborations, with exposures of $\mathcal{E} = 3 \times 10^4$ and 3×10^5 kg day it would be possible to measure the mass of a light [$m_\chi \sim \mathcal{O}(50 \text{ GeV})$] WIMP with an accuracy of roughly 25% and 10% respectively. These numbers, and the upper limits in particular, increase with increasing WIMP mass, and for heavy WIMPs ($m_\chi \gg 100 \text{ GeV}$) even with a large exposure it will only be possible to place a lower limit on the mass. For very light WIMPs, $m_\chi < \mathcal{O}(20 \text{ GeV})$, the number of events above the detector energy threshold would be too small to allow the mass to be measured accurately. If $\sigma_p = 10^{-9}$ pb, with an exposure of $\mathcal{E} = 3 \times 10^5$ kg day it will be possible to measure the mass with an accuracy of $\sim \pm 20\%$ ($^{+100\%}_{-30\%}$) for $m_\chi^{\text{in}} = 50$ (100) GeV. If $\sigma_p = 10^{-10}$ pb, for $m_\chi^{\text{in}} = 50$ GeV, even with an exposure of $\mathcal{E} = 3 \times 10^5$ kg day it will only be possible to determine the WIMP mass to within a factor of a few and for more massive WIMPs it will only be possible to place a lower limit on the mass.

The energy threshold, E_{th} , and the maximum energy, E_{max} , above which recoils are not detected/analysed also affect the accuracy with which the WIMP mass can be determined. Increasing E_{th} (or decreasing E_{max}) not only reduces the number of events detected, but also reduces the range of recoil energies and the accuracy with which the characteristic energy of the energy spectrum, E_{R} , and hence the WIMP mass, can be measured. The effect of increasing E_{th} is smallest for intermediate WIMP masses. For light WIMPs the small E_{R} means that the expected number of events decreases rapidly as the energy threshold is increased, while for heavy WIMPs the large E_{R} , and flatter energy spectrum, means that the smaller range of recoil energies reduces the accuracy with which E_{R} can be measured. The effect of reducing the maximum energy (from infinity to 100 keV) is very small for light WIMPs as the differential event rate above $E_{\text{max}} = 100$ keV is negligible, however for heavy WIMPs the fractional mass limits can

change by $\mathcal{O}(10\%)$.

The relative capabilities of different detectors to determine the WIMP mass depend not only on the WIMP and target masses, but also on their energy thresholds. The WIMP and target mass dependence of the characteristic energy scale of the recoil spectrum suggests that heavy targets will be able to measure the mass of a heavy WIMP more accurately, however the rapid decrease of the nuclear form factor with increasing momentum transfer which occurs for heavy nuclei means that this is in fact not the case.

If the WIMP distribution on the ultra-local scales probed by direct detection experiments is smooth, then the uncertainties in the detailed shape of the local velocity distribution lead to relatively small changes in the shape of the differential event rate [17, 18], and hence a relatively small, [$\mathcal{O}(5\%)$], systematic uncertainty in the WIMP mass [10]. There is however an uncertainty in the local circular speed, v_c , (and hence the typical speed of the WIMPs) of order $\pm 20 \text{ km s}^{-1}$ [15] and since E_R depends on both m_χ and v_c this leads to a degeneracy between m_χ and v_c [10]. For deviations of $\pm 20 \text{ km s}^{-1}$ in the underlying value of v_c this systematic error increases with increasing m_χ^{in} from $\sim 10\%$ for small m_χ^{in} to $\sim 40\%$ for $m_\chi \approx 200 \text{ GeV}$.

The assumption of a smooth WIMP distribution may not be valid on the sub milli-pc scales probed by direct detection experiments (see discussion in Paper I [10]). If the ultra-local WIMP distribution consists of a finite number of streams (with a priori unknown velocities) then the recoil spectrum will consist of a number of (sloping due to the energy dependence of the form factor) steps. The positions of the steps will depend on the stream velocities, the target mass and the WIMP mass. In this case multiple targets would be needed to extract any information on the WIMP mass. Drees and Shan [11] have recently demonstrated that with multiple targets it is in principle possible to constrain the WIMP mass without making any assumptions about the WIMP velocity distribution.

Future experiments aim to have negligible backgrounds, however, non-negligible neutron backgrounds would lead to errors in the determination of the WIMP mass. The size of the errors will depend on the amplitude and shape of the background spectrum. If the background rate is not negligible compared with the WIMP event rate it will be difficult to disentangle a WIMP signal (and the WIMP mass) from the background if the background spectrum has a similar shape to the WIMP spectrum (i.e. exponential background, or flat background with a heavy WIMP). The uncertainties from backgrounds could be mitigated by using multiple targets (see e.g. Ref. [26]), however detectors composed of very different targets (such as Ge and Xe) would be unlikely to have the same background spectra.

Acknowledgments

AMG is supported by STFC and is grateful to Ben Morgan for useful discussions and Marcela Carena for encouragement to investigate some of the issues considered.

5. References

- [1] M. Tegmark et al., Phys. Rev. D **69** 103501 (2004), [astro-ph/0310723](#); S. Cole et al., Mon. Not. Roy. Astron. Soc. **362**, 505 (2005), [astro-ph/0501174](#); J. Dunkley et al., [arXiv:0803.0586](#).
- [2] G. Jungman, M. Kamionkowski and K. Griest, Phys. Rep. **267**, 195 (1996).
- [3] L. Bergström, Rept. Prog. Phys. **63**, 793 (2000), [hep-ph/0002126](#); G. Bertone, D. Hooper and J. Silk, Phys. Rep. **405** 279 (2005), [hep-ph/0404175](#).
- [4] M. W. Goodman and E. Witten, Phys. Rev. D **31**, 3059 (1985).
- [5] L. Baudis, [arXiv:0711.3788](#) (2007).
- [6] J. D. Lewin and P. F. Smith, Astropart. Phys. **6**, 87 (1996).
- [7] M. J. Lewis and K. Freese, Phys. Rev. D **70** 043501 (2004), [astro-ph/0307190](#).
- [8] J. L. Bourjaily and G. L. Kane, [hep-ph/0501262](#).
- [9] http://particleastro.brown.edu/theses/060421_Monte_Carlo_Simulations_Dark_Matter_Detectors_Jackson_v3.pdf;
http://cosmology.berkeley.edu/inpac/CDMSCE_Jun06/Talks/200606CDMSCEmass.pdf
- [10] A. M. Green, JCAP08(2007)022, [hep-ph/0703217](#).
- [11] M. Drees and C-L. Shan, [arXiv:0803.4477](#) (2008).
- [12] D. Hooper and E. A. Baltz, [arXiv:0802.0702](#) (2008); N. Bernal, A. Goudelis, Y. Mambrini and C. Munoz, [arXiv:0804.1976](#) (2008); B. Altunkaynak, M. Holmes and B. D. Nelson, [arXiv:0804.2899](#) (2008).
- [13] R. W. Schnee et al., proceedings of DARK 2004, fifth international Heidelberg conference on dark matter in Astro and Particle Physics, [astro-ph/0502435](#) (2004); P. L. Brink et al., proceedings of Texas Symposium on Relativistic Astrophysics, [astro-ph/0503583](#) (2004).
- [14] R. H. Helm, Phys. Rev. **104** 1466 (1956).
- [15] F. J. Kerr and D. Lynden-Bell, Mon. Not. Roy. Astron. Soc. **221**, 1023 (1986).
- [16] M. C. Smith et al., Mon. Not. Roy. Astron. Soc. **379**, 755 (2007), [astro-ph/0611671](#).
- [17] M. Kamionkowski and A. Kinkhabwala, Phys. Rev. D **57**, 3256 (1998), [hep-ph/9710337](#); F. Donato, N. Fornengo and S. Scopel, Astropart. Phys. **9**, 247 (1998), [hep-ph/9803295](#).
- [18] A. M. Green, Phys. Rev. D **66**, 083003 (2002), [astro-ph/0207366](#).
- [19] B. Moore et al., Phys. Rev. D **64** 063508 (2001), [astro-ph/0106271](#); S. Stiff and L. Widrow, Phys. Rev. Lett. **90**, 211301 (2003), [astro-ph/0301301](#).
- [20] A. Helmi, S. D. M. White and V. Springel, Phys. Rev. D **66**, 0635023 (2002), [astro-ph/0201289](#); M. Vogelsberger et al., [arXiv:0711.1105](#).
- [21] Z. Ahmed et al., [arXiv:0802.3530](#) (2008).
- [22] J. Angle et al., Phys. Rev. Lett. **100**, 021303 (2008), [arXiv:0706.0039](#).
- [23] G. Cowan, *Statistical data analysis*, published by Oxford University Press (1998).
- [24] D. S. Akerib et al., Phys. Rev. D **72**, 052009 (2005), [astro-ph/0507190](#).
- [25] M. J. Carson et al., NIMA **546**, 509 (2005); L. Kaufmann and A. Rubbia, [hep-ph/0612056](#); H.S. Lee et al. NIMA **571**, 644 (2007).
- [26] H. Kraus et al., Phys. Lett. B **610** 37 (2005).